Supplemental Figures

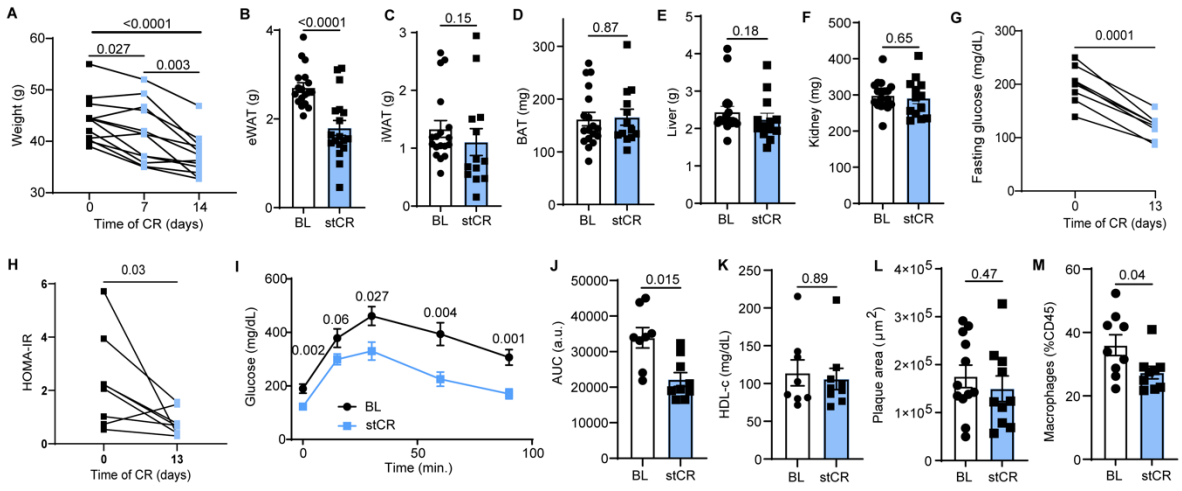

Supp. Fig. 1: stCR promotes weight loss and improves metabolic parameters.

(A) Body weight assessed during caloric restriction. (B-F) Tissue weights at the end of the experiment: (B) eWAT, (C) iWAT, (D) BAT, (E) liver (F) and kidney. (G) Fasting glucose levels at baseline and after stCR. (H) Homeostatic Model Assessment for Insulin Resistance (HOMA-IR) at baseline and after stCR. (I, J) Glucose tolerance test performed in baseline vs. caloric restricted mice. (K) HDL-C measurements. (L) Total plaque area quantified in root sections. (M) Proportion of macrophages from all white blood cells in aortic arches, measured by flow-cytometry. P-values were determined via (A) one-way ANOVA with Tukey's multiple comparisons test, (B, F-L) two-tailed Student's t-test and (C-E, M) Mann-Whitney test.

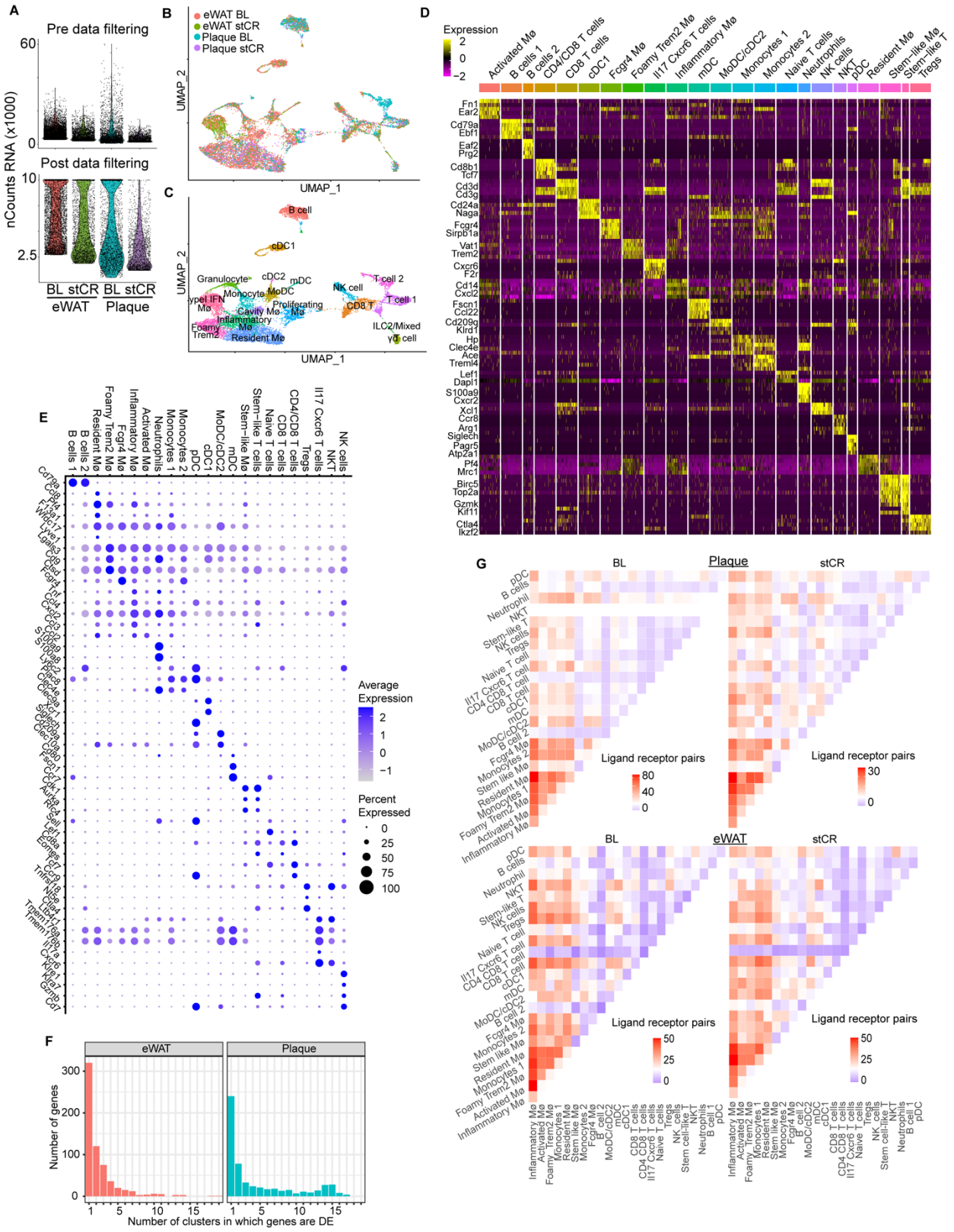
A
Pre data filtering
Post data filtering
nCounts RNA (x1000)
BL stCR BL stCR
eWAT Plaque
B
eWAT BL
eWAT stCR
Plaque BL
Plaque stCR
UMAP_1
UMAP_2
C
B cell
cDC1
Granulocyte
cDC2
mDC
Monocyte
MoDC
Type I IFN Mø
Cavity Mø
Prolifecating Mø
NK cell
CD8 T
T cell 2
T cell 1
Inflammatory Mø
Foamy Trem2 Mø
Resident Mø
ILC2/Mixed γδ T cell
D
Expression
Activated Mø
B cells 1
B cells 2
CD4/CD8 T cells
CD8 T cells
cDC1
Fcgr4 Mø
Foamy Trem2 Mø
Il17 Cxcr6 T cells
Inflammatory Mø
mDC
MoDC/cDC2
Monocytes 1
Monocytes 2
Naive T cells
Neutrophils
NK cells
NKT
pDC
Resident Mø
Stem-like Mø
Stem-like T
Tregs
E
Average Expression
Percent Expressed
F
eWAT
Plaque
Number of genes
Number of clusters in which genes are DE
G
BL
Plaque
stCR
eWAT
Ligand receptor pairs

Supp. Fig. 2: Single-cell RNA-seq of plaque and eWAT leukocytes in obesity and weight loss.

(A) Quality control of scRNAseq data pre- and post-filtering for cells containing >10,000 unique RNA reads (see methods). UMAPs color coded by (B) sample type and (C) closest match compared to Zernecke et al. (D) Top 5 marker genes per cluster. (E) Expression of marker genes defined by Zernecke et al., used to annotate leukocyte clusters in our dataset. (F) Number of clusters with shared DEGs (comparing stCR and BL) in eWAT (red) and plaques (blue). (G) Cell-cell interaction analysis, presenting the number of receptor-ligand pairs across all clusters in plaque (top) and eWAT (bottom) in obese (left) and stCR (right).

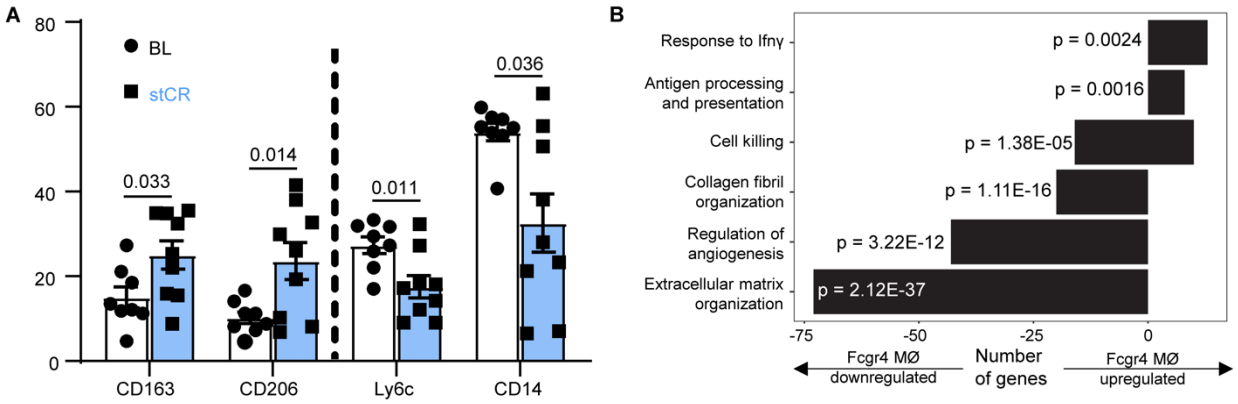

Supp. Fig. 3: stCR induces a less inflammatory, pro-resolving phenotype of plaque macrophages, partly through induction of *Fcgr4*+ macrophages.

(A) Flow cytometry analysis of plaque macrophages after aortic arch digestion (n=8-10). P-values were determined via two-tailed Student's t-test except for CD14, which was determined by Mann-Whitney test. (B) GO pathways increased and repressed in FCGR4+ macrophages ("Fcgr4 MΦ") from adipose tissue following caloric restriction. Enriched GO terms have adjusted p-value < 0.05.

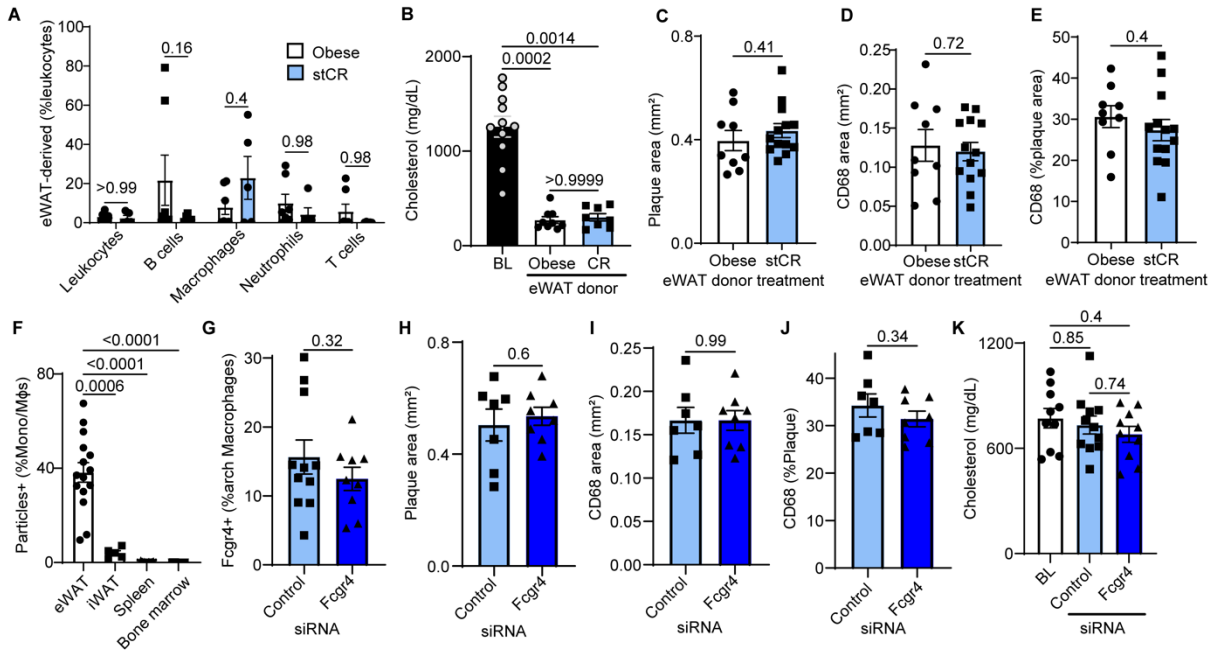

Supp Fig. 4: *Fcgr4*+ macrophages from eWAT reduce plaque necrotic core, but do not change plaque macrophage content.

(A) Flow cytometry analysis of plaque leukocytes of eWAT recipient mice, 2 weeks after transplantation (n=5-6). (B) Plasma cholesterol at tissue harvest. (C) Quantification of total plaque area and (D-E) macrophage content in aortic root sections (n=7-11). (F) Flow cytometry analysis of particle engulfment by macrophages from different tissues (n=5-12). (G) Flow cytometry analysis of FCGR4+ macrophages (Fcgr4+ on Y-axis) in aortic arch of mice receiving either control or *Fcgr4* siRNA-containing particles (n=9-12). (H) Quantification of total plaque area and (I-J) macrophage content of aortic root sections, after injections of control or *Fcgr4* siRNA particles. (K) Plasma cholesterol after 2 weeks of siRNA-carrying particle treatment. P-values were determined via (A) two-way ANOVA with Sidak (F,K) one-way ANOVA with Tukey's multiple comparisons test, (E) Kruskal-Wallis with Dunn's multiple comparisons test and (B-D, G-J) two-tailed Student's t-test.

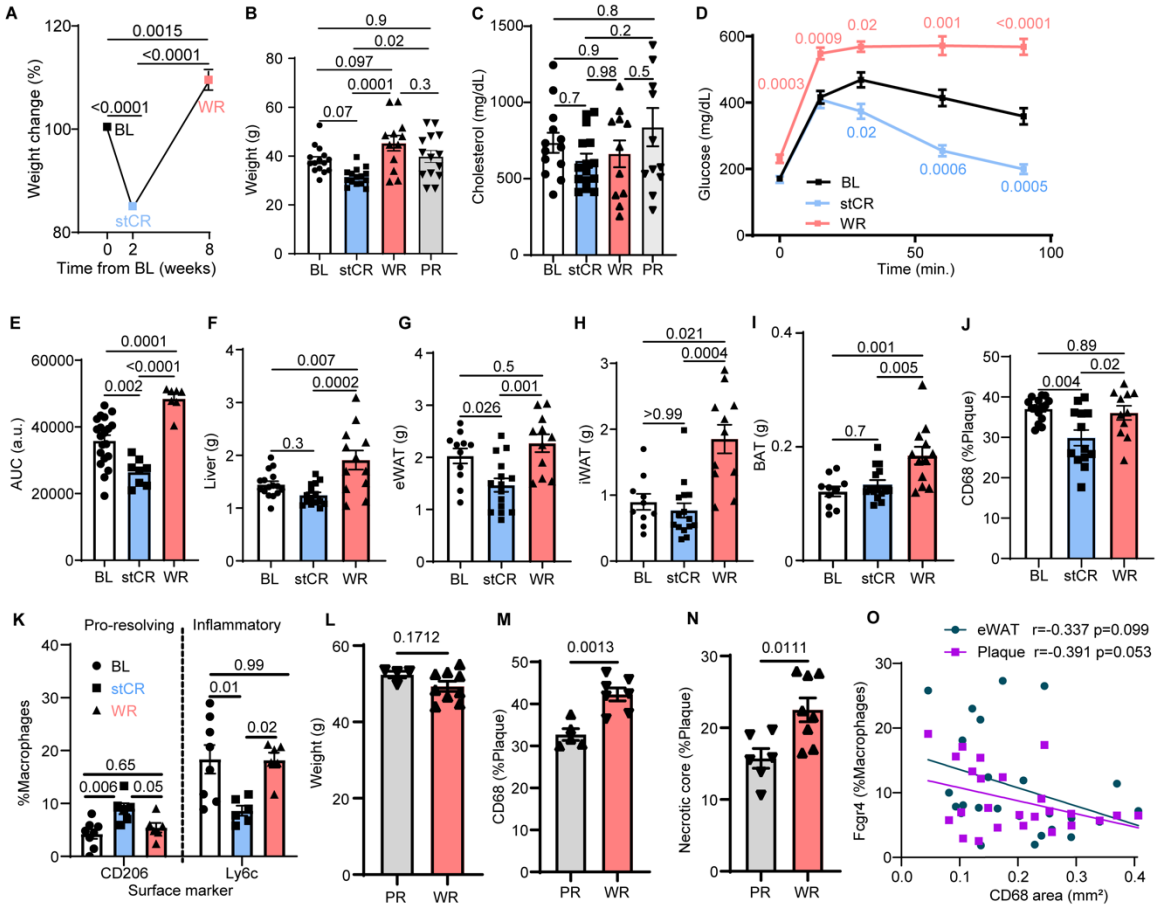

Supp. Fig. 5: Weight regain worsens metabolic parameters and plaque inflammation.

(A) Percent body weight change during weight cycling, n=29. (B) Body weight and (C) plasma cholesterol levels of all groups at harvest. (D, E) Glucose tolerance test performed in baseline, stCR and weight regain groups, n=7-20. (F-I) Tissue weights at the end of the experiment: (F) liver, (G) eWAT, (H) iWAT, (I) BAT. (J) Macrophage percentage of total plaque area measured in aortic root sections. (K) Flow cytometry analysis of aortic arch macrophages. (L) Body weights (M) CD68 and (N) necrotic core content in a separate cohort of mice harvested after 3 weeks of weight regain and

compared to mice that did not weight cycle (n=6-8). (O) Simple linear regression showing correlation between *Fcgr4*+ macrophages (Fcgr4 on Y-axis) from eWAT and plaques with total macrophage content in plaques. P-values were determined via (A-G, K) one-way ANOVA with Tukey's multiple comparisons test, (H) Kruskal-Wallis with Dunn's multiple comparisons test, (L-M) student t-test and (N) simple linear regression analysis.

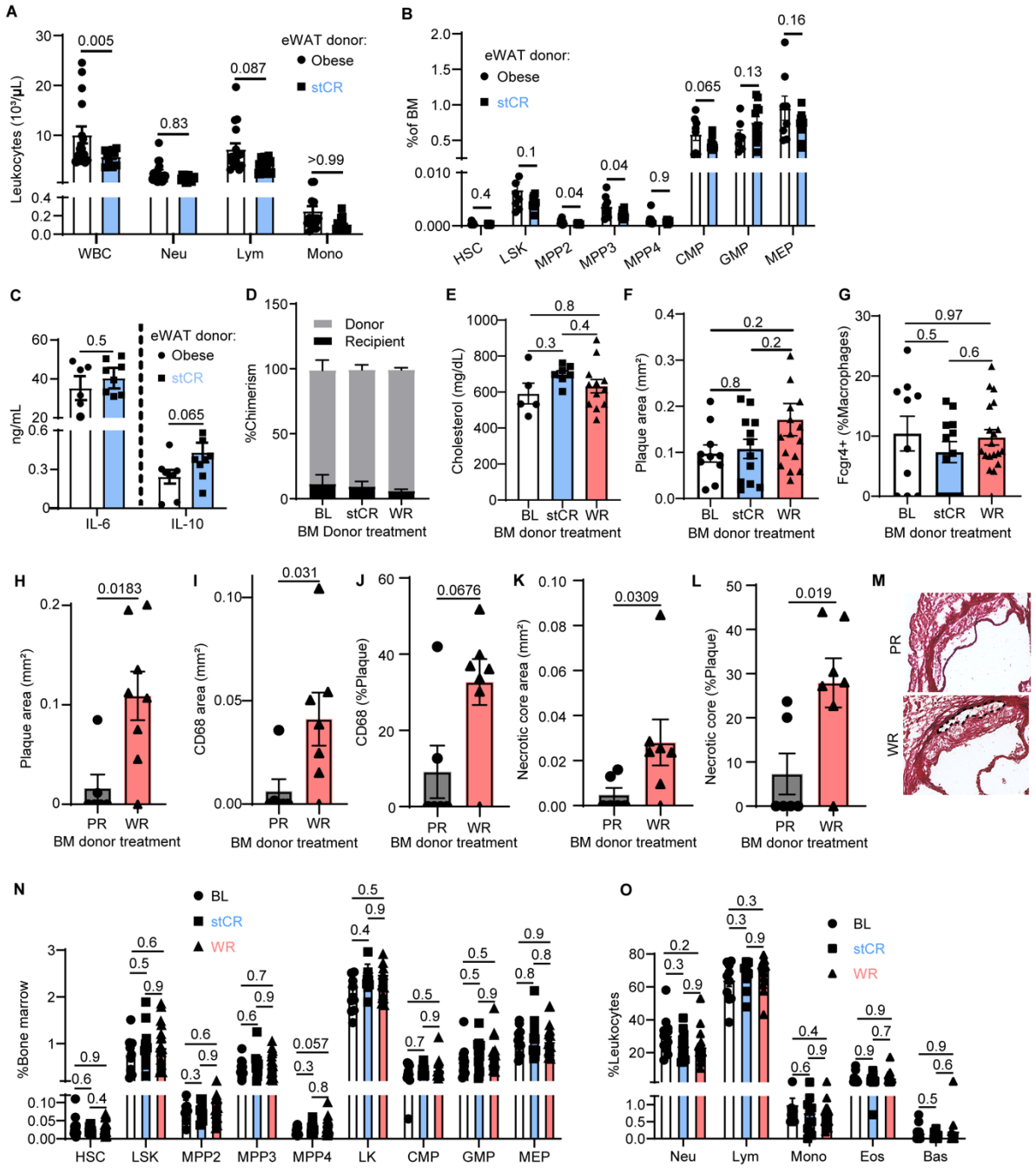

Supp. Fig. 6: Weight cycling induces long-term reprogramming of hematopoietic progenitors.

(A) Abundances of circulating white blood cells and (B) their bone marrow progenitors in mice transplanted with eWAT from obese and stCR donors (Fig. 4A). (C) Cytokines produced by bone marrow cells harvested from mice transplanted with obese or stCR

eWAT and treated ex vivo with LPS for 16h, n=6-8. (D) Engraftment frequencies of donor cells following BM transplantation, n=6-8. (E) Plasma cholesterol at the end of BM transplantation experiment, n=5-10. (F) Total plaque area of mice transplanted with BL, stCR and WR bone marrows and fed HFHC diet for 14 weeks. (G) Flow cytometry analysis of FCGR4+ macrophages in plaques, n=8-14. (H-M) Bone marrow transfer studies were repeated, with donors either continuously fed ad libitum (PR), or subjected to the weight cycling protocol (as in Fig. 6D; n=6-7). Recipient mice were harvested after 14 weeks of HFHC diet feeding and aortic root sections assessed for (H) plaque area, (I-J) macrophage content and (K-M) necrotic core content. (N) Frequencies of bone marrow hematopoietic stem and progenitor cells and (O) circulating white blood cells were analyzed at the end of the bone marrow transplantation experiment. P-values were determined via (A, B, O) two-way ANOVA with Sidak multiple comparison test, (C) two-tailed Student's t-test, (J-N) Mann-Witney test, and (E-G) one-way ANOVA with Tukey’s multiple comparisons test.

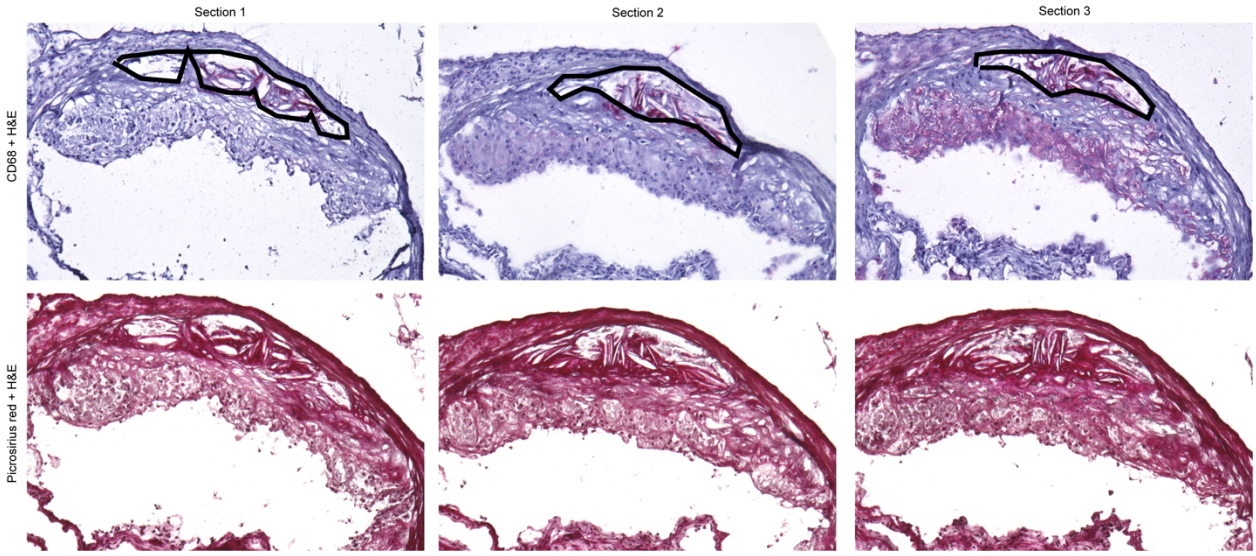

Supp. Fig. 7: Necrotic core quantification.

Adjacent sections (6μm apart) of aortic roots were stained for H&E together with either CD68 (top row) or picrosirius red (bottom row). Areas lacking both nuclei and extracellular matrix were defined as necrotic core (outlined in black). The picrosirius red images were used to confirm the necrotic core area selection in the CD68-stained slides, then used for quantification. Serial sections spanning >400μm were quantified per mouse.